

Vorticity and the Nernst Effect in Cuprate Superconductors

N. P. Ong¹, Yayu Wang¹, S. Ono², Yoichi Ando², and S. Uchida³

¹Department of Physics, Princeton University, Princeton, New Jersey 08544, USA

²Central Research Institute of Electric Power Industry, Komae, Tokyo 201-8511, Japan

³School of Frontier Sciences, University of Tokyo, Tokyo 113-8656, Japan

(Dated: June 28, 2021)

We present a review of the vortex-Nernst effect in the 3 cuprate families $\text{La}_{2-x}\text{Sr}_x\text{CuO}_4$, $\text{Bi}_2\text{Sr}_2\text{CaCu}_2\text{O}_8$, and $\text{YBa}_2\text{Cu}_3\text{O}_y$, and discuss the scenario that the superconducting transition in the hole-doped cuprates corresponds to the destruction of long-range phase coherence rather than the vanishing of the order-parameter amplitude.

PACS numbers: 74.40.+k, 72.15.Jf, 74.72.-h

In conventional superconductors, the amplitude of the complex order parameter $\hat{\Psi}(\mathbf{r}) = |\Psi|e^{i\theta(\mathbf{r})}$ vanishes as the temperature $T \rightarrow T_{c0}^-$ where T_{c0} is the zero-field critical temperature. Concurrently, *long-range* phase coherence also vanishes at T_{c0} . In an alternate scenario, phase coherence may vanish at T_{c0} , but $|\Psi|$ remains finite to temperatures significantly higher than T_{c0} . An extreme example is the Kosterlitz Thouless (KT) transition [1] in 2D superconductors. Although the cuprates are intrinsically 3D systems, evidence has accumulated over the years that their transition to superfluidity reflects the loss of phase coherence rather than the vanishing of $|\Psi|$. Early μSR experiments [2] showed that T_{c0} scales linearly with the superfluid density in the underdoped regime. In thin-film samples, kinetic inductance is observed to persist to ~ 25 K above T_{c0} [3]. A series of Nernst experiments [4, 5, 6, 7, 8, 9, 10] has provided perhaps the firmest evidence that the transition in zero field corresponds to rapid proliferation of mobile vortices which destroy phase coherence [11, 12]. We review these results here.

In the vortex-liquid state, a temperature gradient $-\nabla T \parallel \hat{\mathbf{x}}$ induces vortices to flow with velocity $\mathbf{v} \parallel \hat{\mathbf{x}}$ (the field $\mathbf{B} \parallel \hat{\mathbf{z}}$). As the vortices cross a reference line parallel to $\hat{\mathbf{y}}$, stochastic phase slips generate a *dc* voltage V_J via the Josephson equation $2eV_J = 2\pi\hbar\dot{n}_v$, which translates to a weak electric field $E_y = Bv$ antisymmetric in \mathbf{B} (here \dot{n}_v is the average number of vortices crossing the line per second). The Nernst signal, defined as $e_y = E_y/|\nabla T|$, has turned out to be a powerful probe of the existence of vorticity in the phase diagram of the cuprates [4, 5]. A recent theoretical discussion may be found in Ref. [13].

In cuprates, $e_y(T, H)$ exists as a strong signal over a rather large region in the T - H (temperature-field) plane.

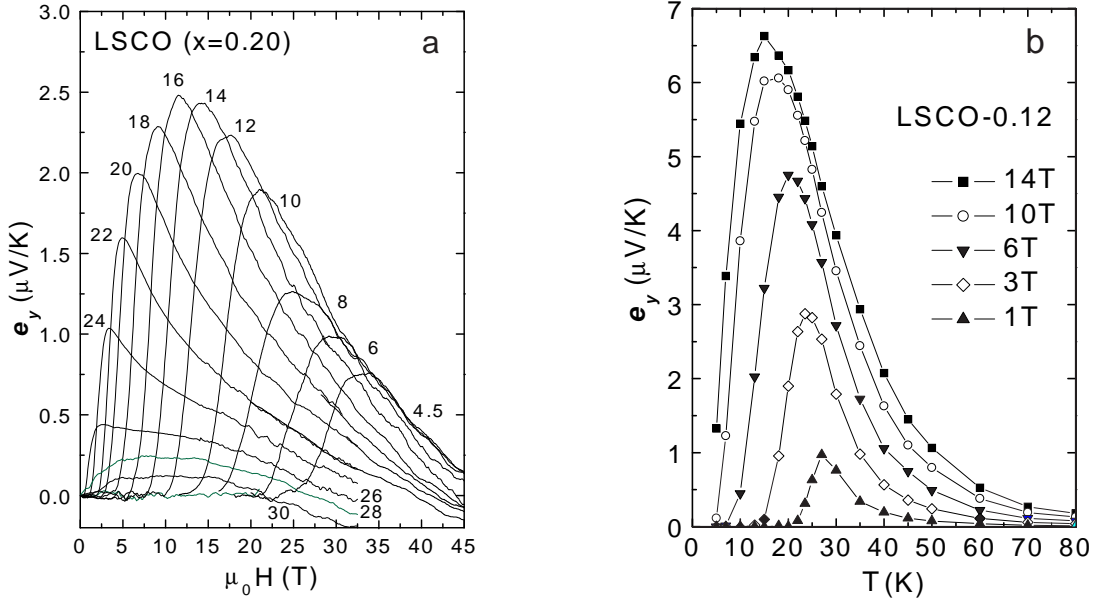


FIG. 1: (a) The observed Nernst signal $e_y = E_y/|\nabla T|$ vs. field H up to 45 T in overdoped LSCO at selected T ($x = 0.20$, $T_{c0} = 28$ K). The prominent peak and decrease at high fields are the vortex Nernst signal. At $T \lesssim 18$ K, the Nernst signal of the holes which is negative causes e_y to become slightly negative at high fields. (b) The T dependence of e_y at fixed H in underdoped LSCO ($x = 0.12$). Note the continuity of the signal across the transition $T_{c0} = 28.9$ K.

Figure 1a shows plots of e_y vs. H in overdoped $\text{La}_{2-x}\text{Sr}_x\text{CuO}_4$ (LSCO) in which $x = 0.20$ and $T_{c0} = 28$ K. The characteristic ‘tent’ profile of the curve of e_y vs. H below T_{c0} becomes apparent only in very high fields [6, 7]. The profile is strikingly similar to that observed in the Abrikosov state of low- T_c type II superconductors. Starting at the lowest T (4.5 K), we see that e_y is zero until the solid-liquid melting transition occurs at H_m (~ 25 T). In the liquid state, e_y rises to a maximum value before decreasing monotonically towards zero at a field that we identify with the upper critical field $H_{c2} \simeq 50$ T (the field at which the pairing amplitude is completely suppressed). As T increases, both H_m and the peak field H^* move to lower field values. Both the peak feature as well as the monotonic decrease towards zero become increasingly dramatic as T is increased to the interval 10 to 20 K. A complication in overdoped LSCO is that the hole carriers contribute a moderately large, negative Nernst signal [5]. Close to T_{c0} , this carrier contribution pulls the vortex signal to negative values in high fields. (We define [5] the Nernst signal to be positive if the observed E -field is consistent with a vortex origin, i.e. given by $\mathbf{E} = \mathbf{B} \times \mathbf{v}$.) The hole contribution complicates the task of isolating the vortex signal at high T in overdoped samples, but is negligible for $x \leq 0.17$.

A different perspective on $e_y(T, H)$ is shown in Fig. 1b in underdoped LSCO ($x = 0.12$, $T_{c0} = 28.9$ K). Each curve represents the profile of e_y vs. T at fixed field. At this doping, the hole contribution to e_y is negligibly small compared with the vortex signal. The important feature here is that e_y extends continuously to T high above T_{c0} . There is no sign of a sharp boundary separating the vortex liquid state at low T and H from a high- T ‘normal state’. Displaying the data in this way brings out clearly the smooth continuity of the vortex signal above and below T_{c0} . This continuity is also apparent in contour plots of $e_y(T, H)$ in the T - H plane, as reported in Ref. [6, 8] (see Fig. 3b as well).

Of all the cuprates, the Bi-based families display the weakest carrier-Nernst signals. Figure 2 shows the total e_y measured at 14 T in underdoped $\text{Bi}_2\text{Sr}_2\text{CaCu}_2\text{O}_8$ (Bi 2212) and overdoped Bi 2212 [Panels (a) and (b), respectively]. In both cases, the hole signal is negative and always less 100 nV/K in magnitude (at 14 T). In the underdoped sample (Panel a), the vortex signal appears at 120 K and increases rapidly to a peak value of $2.6 \mu\text{V}/\text{K}$ near $T_{c0} = 50$ K (the Meissner response is shown by the open circles). Hence there exists a 70 K interval over which vortex fluctuations are readily observed. In the overdoped sample (b), the onset is at 100 K whereas $T_{c0} = 77$ K. The fluctuation regime is narrower in the overdoped regime (this trend is shared by LSCO), but it still extends over a 23-K interval.

We next discuss Nernst results in $\text{YBa}_2\text{Cu}_3\text{O}_y$ (YBCO). Because overdoped YBCO is known to have the smallest anisotropy of all the cuprates, it is interesting to examine its fluctuation regime. Figure 3a displays curves of e_y vs. H at temperatures 74 to 94 K for an untwinned YBCO crystal with $y = 6.99$ and $T_{c0} = 93$ K with $-\nabla T \parallel \hat{\mathbf{b}}$. In contrast to LSCO and Bi 2212, the increase in e_y at the melting line is nearly vertical. In Fig. 3b, we display the variation of $e_y(T, H)$ in the T - H plane as a contour plot (for optimally-doped YBCO with $y = 6.95$). The solid lines are contours of e_y with the values given in the left-hand column. The melting field H_m is shown as a white curve. To the left of $H_m(T)$, the black region represents the vortex-solid phase, in which $e_y = 0$. A striking feature of the

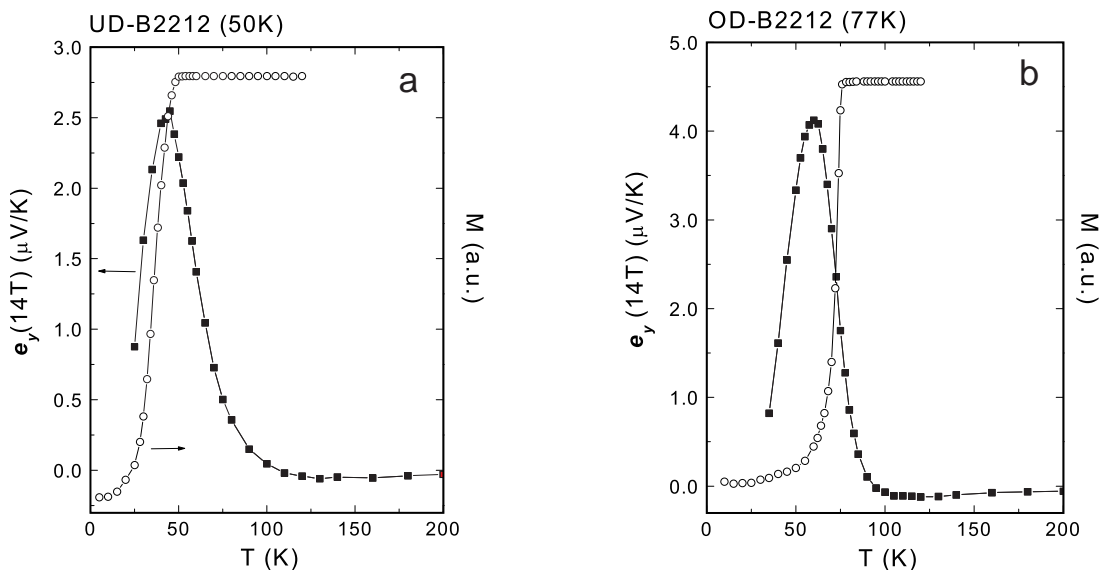


FIG. 2: Comparison of the Nernst signal e_y measured at 14 T (solid symbols) in underdoped Bi 2212 (Panel a) and overdoped Bi 2212 (b). The diamagnetic susceptibility χ measured with $H = 10$ Oe (open symbols) shows the sharp Meissner transition at 50 K and 77 K in the 2 crystals, respectively. Above T_v (onset of the vortex signal), the carrier contribution to e_y is weak (< 100 nV/K at 14 T) and negative.

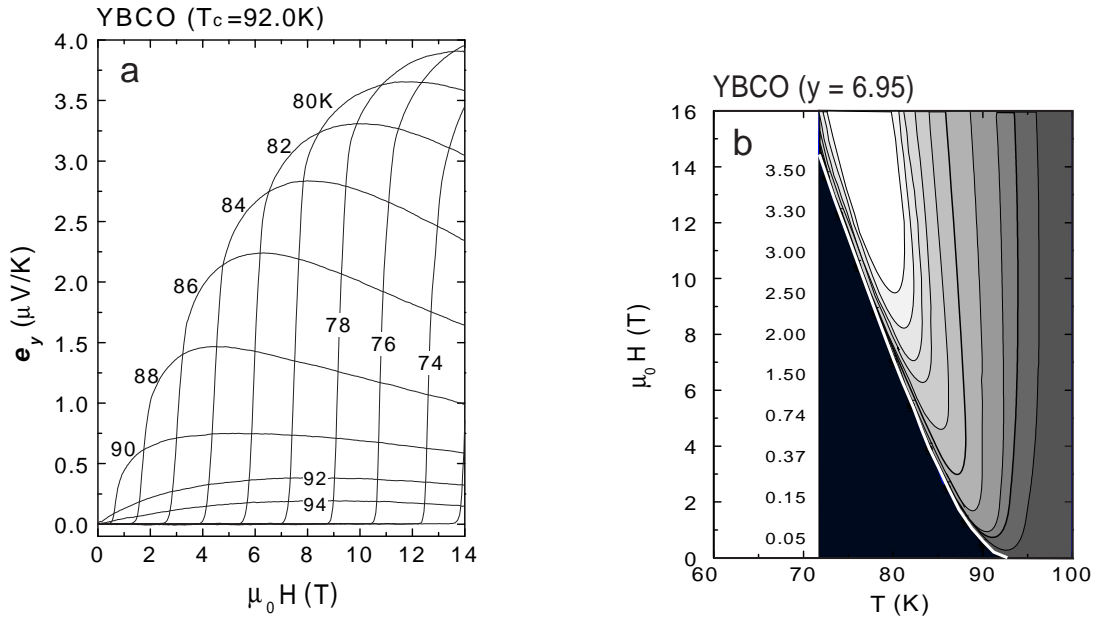


FIG. 3: (a) Curves of e_y vs. H in untwinned YBCO ($y = 6.99$, $T_{c0} = 93$ K) with $-\nabla T \parallel \mathbf{b}$ from 74 to 94 K. (b) The contour plot of $e_y(T, H)$ in the T - H plane of optimally doped YBCO ($y=6.95$) with contour values indicated on the left column (in $\mu\text{V/K}$). $H_m(T)$ (white curve) separates the vortex solid phase (shaded black) from the liquid phase. The vortex Nernst signal onset is $T_{\text{onset}} \simeq 105$ K.

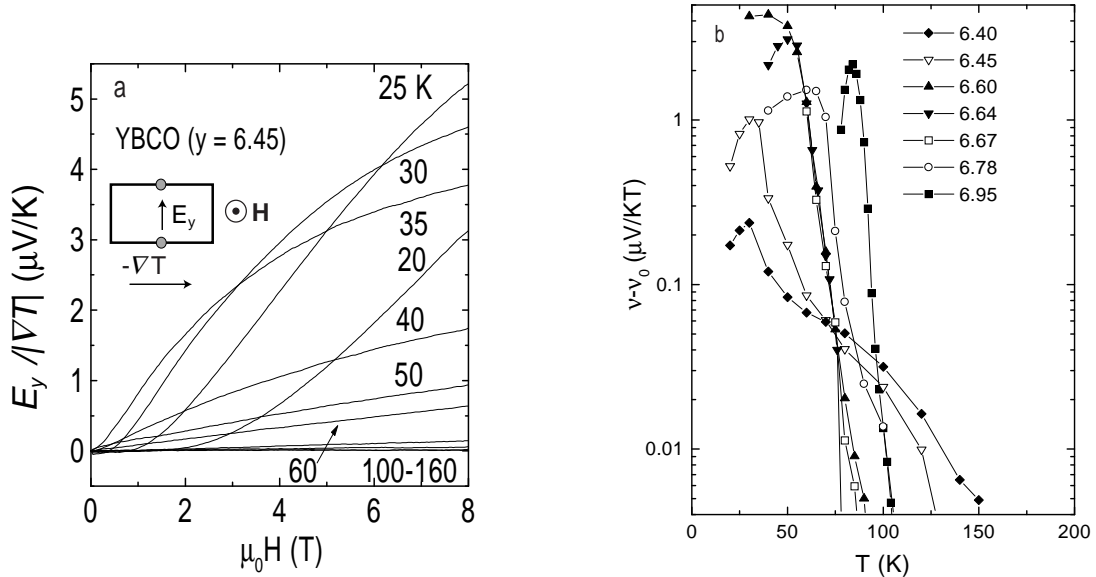


FIG. 4: (a) Curves of e_y vs. H in underdoped YBCO ($y = 6.45$, $T_{c0} = 45$ K) from 20 to 160 K. (b) The vortex Nernst coefficient $\nu - \nu_N$ (with hole signal subtracted) plotted vs. T in a series of YBCO crystals ($y = 6.40$ to 6.95). In the doping interval $6.60 < y < 6.80$, ν_N is relatively large and negative above T_{c0} (see text).

contour plot is that even in optimal YBCO, the fluctuation regime is present although it is quite narrow (~ 10 K). As we decrease the oxygen content y , the fluctuation regime expands significantly, again in agreement with the trend in LSCO and Bi 2212. Figure 4a displays curves of e_y vs. H for an underdoped YBCO ($y = 6.45$) in which the vortex signal extends to above 100 K even though $T_{c0} = 45$ K. At temperatures above T_{c0} where e_y is nearly linear in H for fields below 14 T, it is convenient to represent the Nernst magnitude by the initial slope $\nu = e_y/H$ (the Nernst coefficient). Figure 4b displays how ν (with the carrier contribution ν_N subtracted) varies with T in 7 crystals of YBCO over a broad range of y . Above T_{c0} , the vortex Nernst coefficient $\nu - \nu_N$ falls monotonically with a slope that depends monotonically on the oxygen content. As y decreases from 6.95, the slope becomes progressively weaker until

in the sample with $y = 6.40$, the fluctuation regime extends to 140 K. There exists a feature of the Nernst effect in YBCO that is not seen in the other hole-doped cuprates examined to date (LSCO, Bi 2201, Bi 2212 and Tl 2201). In a narrow range of doping $6.60 < y < 6.80$, the Nernst coefficient ν is strongly negative in a 10-20 K interval above T_{c0} . This negative contribution possibly arises from holes in the chains. As shown in Fig. 4b, in the doping range $6.60 < y < 6.80$, the negative contribution causes $\nu - \nu_N$ to fall very steeply. We believe this may be an artifact of an unsatisfactory subtraction procedure. As we further decrease y (< 6.60), this negative contribution abruptly disappears, and we recover a pattern more similar to that in the other hole-doped cuprates.

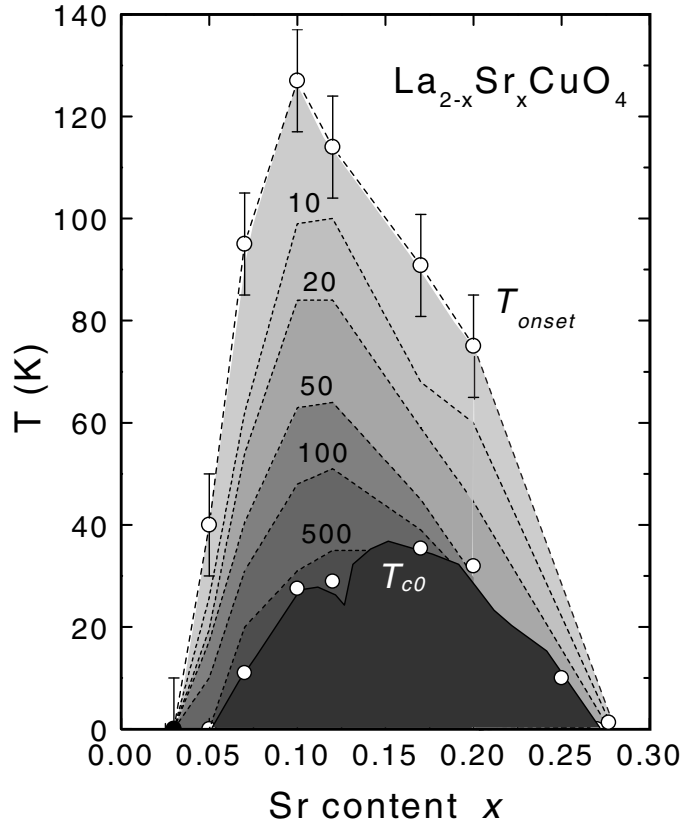


FIG. 5: Phase diagram of LSCO showing contour lines of the vortex Nernst signal observed above T_{c0} (ν at each contour is given in nV/KT). Note that the highest temperature occurs near $x = 0.10$ (rather than 0.15) in all contours. The vortex-Nernst signal is not observed in the samples at $x = 0.26$ and 0.03.

Discussion The Nernst measurements, which are most extensive in LSCO, provide the following picture of the fluctuation regime above T_{c0} . The phase diagram for LSCO shown in Fig. 5 has been pieced together from results obtained in 8 crystals (see Refs. [4, 5, 6, 7]). The vortex excitation state (shaded) extends upwards to high temperatures above T_{c0} deep into the pseudogap state.

We note that the vortex signal is strictly confined to the doping interval ($0.03 < x < 0.26$) in which superconductivity is observed (the right anchor at $x = 0.26$ is a recently studied crystal in which no vortex signal is observed at any H and T). This precludes other origins for e_y such as density-wave excitations in the ordered AF state on the underdoped side or Fermi-liquid excitations on the overdoped side.

As we cool a sample (with $x = 0.12$, for e.g.) from high T , it first crosses into the pseudogap state at $T^* \sim 300$ K. Starting at 115 K, strong fluctuations appear between the pseudogap state and d -wave superconducting (dSC) state. The existence of short-lived superconducting regions with short-range phase rigidity and vorticity leads to a weak vortex-Nernst signal. As T decreases from 115 K to $T_{c0} = 29$ K, e_y increases steeply (nominally as T^{-2}) with rapid expansion of the fluctuating regions. However, at high T , bulk diamagnetism is virtually undetectable, even as a weak fluctuation signal. We believe this is a consequence of the weak phase stiffness at long length scales in this vortex fluctuation phase. Starting about 10 K above T_{c0} , one may finally observe a rapidly divergent bulk diamagnetism signal as the Meissner transition T_{c0} is approached and long-range phase coherence spreads throughout the sample (provided H is zero or very weak). A characteristic of the cuprates is that the vortex Nernst signal is observed high above the temperature at which conventional fluctuating diamagnetism can be detected. As apparent in Fig. 1b, at

moderately strong field, e_y continues to increase smoothly through T_{c0} , attaining a maximum at lower T . Below the peak temperature, e_y decreases steeply as the vortices become less and less mobile close to the melting line.

Broadly speaking, there seem to be 3 viewpoints regarding the nature of the pseudogap state: 1) It is simply a strongly fluctuating superconducting state with complete absence of long-range phase coherence. 2) It has an entirely different electronic state from dSC and competes with it for FS area. 3) It is a pairing state that is distinct from dSC, yet closely related to it in terms of symmetry. Our experiments favor the third scenario. The onset of the pseudogap state at T^* is invariably at a much higher T (by a factor of ~ 2) than the Nernst signal onset T_{onset} . Moreover, the field scale for suppressing vorticity H_{c2} , while high, is still significantly lower than field scales associated with suppression of the pseudogap measured by Shibauchi *et al.* [14]. Hence the pseudogap state seems to be distinct in electronic character from dSC. Nonetheless, the vortex fluctuation phase displayed in Fig. 5 implies that fluctuations between them extend over a very broad range of T . The strong fluctuations suggest that the two states are closely related in free energy.

Finally, we return to the nature of the transition at T_{c0} . If we plot H_m vs. T in the T - H plane we find that the melting temperature $T_m(H)$ terminates at T_{c0} , i.e. $T_m(0) = T_{c0}$. In all cuprates, the high-temperature limit of the vortex-solid coincides with the Meissner transition (see for e.g., Fig. 3b). The Nernst picture provides a fresh perspective on this feature. Let us decrease T from high above the melting line with H fixed at 1 Tesla. Initially, the rapidly mobility of the vortices (both spontaneous and field-induced) preclude long-range phase coherence from developing. As soon as the melting line is crossed, the vortices become immobile in the solid phase and long-range phase coherence extends throughout the sample. Now we repeat the cool-down at successively smaller H . Because of the seamless continuity of the vortex-liquid, the same situation obtains in weak fields. In the limit $H = 0$, we initially have equal spontaneous populations of up and down mobile vortices. As we cross the terminal point $T_m(0)$, they become immobile in the vortex solid phase. Hence the occurrence of long-range phase coherence is also associated with the solid-liquid transition just as in finite fields. In all the hole-doped cuprates, we seem to have the situation $T_m(0) > T_{KT}$, where T_{KT} is the intrinsic KT transition transition in the isolated CuO_2 plane with the same hole concentration. In bulk crystals, the 3D melting transition pre-empts the KT transition [8]. The Meissner transition is the point at which the mobile vortices become frozen in the solid phase, rather than a true 2D KT transition.

High-field measurements were performed at the U.S. National High Magnetic Field Lab., Tallahassee, a facility supported by the U.S. National Science Foundation (NSF) and the State of Florida. The research at Princeton is supported by the NSF (Grant DMR DMR 0213706). S. U. and N.P.O. acknowledge partial support from New Energy and Industrial Technol. Development Org. NEDO (Japan).

-
- [1] J. M. Kosterlitz and D. J. Thouless, *J. Phys. C* **6**, 1181 (1973); M. R. Beasley, J. E. Mooij, and T. P. Orlando, *Phys. Rev. Lett.* **42**, 1165 (1979).
 - [2] Y. J. Uemura *et al.*, *Phys. Rev. Lett.* **62**, 2317 (1989).
 - [3] J. Corson, R. Mallozzi, J. Orenstein, J. N. Eckstein, and I. Bozovic, *Nature* **398**, 221 (1999).
 - [4] Z. A. Xu, N. P. Ong, Y. Wang, T. Kakeshita, and S. Uchida, *Nature* **406**, 486 (2000).
 - [5] Yayu Wang *et al.*, *Phys. Rev. B* **64**, 224519 (2001).
 - [6] Yayu Wang, N. P. Ong, Z. A. Xu, T. Kakeshita, S. Uchida, D. A. Bonn, R. Liang, W. N. Hardy, *Phys. Rev. Lett.* **88**, 257003 (2002).
 - [7] Yayu Wang *et al.*, *Science* **299**, 86 (2003).
 - [8] N. P. Ong and Yayu Wang, *Proceedings of the M2S-RIO meeting on Superconductivity* (2003), *Physica C, to appear*; cond-mat/ 0306399.
 - [9] C. Capan *et al.* *Phys. Rev. Lett.* **88**, 056601 (2002).
 - [10] H. H. Wen *et al.*, *Europhys. Lett.* **63**, 583 (2003).
 - [11] V. J. Emery and S. A. Kivelson, *Nature* **374**, 434 (1995).
 - [12] A. K. Nguyen and A. Sudbo, *Phys. Rev. B* **57**, 3123 (1998).
 - [13] Iddo Ussishkin, S. L. Sondhi, and David A. Huse, *Phys. Rev. Lett.* **89**, 287001 (2002).
 - [14] T. Shibauchi, L. Krusin-Elbaum, Ming Li, M. P. Maley, and P. H. Kes, *Phys. Rev. Lett.* **86**, 5763 (2001).